SELF-ROLLED-UP MEMBRANE (S-RUM) CAPACITORS AND FILTERS FOR RADIO FREQUENCY COMMUNICATION

BY

MOYANG LI

THESIS

Submitted in partial fulfillment of the requirements
for the degree of Master of Science in Electrical and Computer Engineering
in the Graduate College of the
University of Illinois at Urbana-Champaign, 2017

Urbana, Illinois

Adviser:

Professor Xiuling Li

Abstract

Self-rolled-up membrane (S-RuM) is a novel technology to build precisely controllable three-dimensional (3D) micro-structures. This technology finds wide applications in passive electronics, photonics, and neural interfaces, and achieves great device size reduction and performance enhancement. For passive electronics, devices based on S-RuM utilize electromagnetic energy well-confined in the device tubular cavity with extremely high efficiency, and break the footprint and parasitic effect limit set by conventional planar devices. S-RuM inductors and capacitors can reach self-resonant frequency up to 60 GHz, Q factor up to 80, and with footprint one hundredth that of the state-of-the-art 2D counterparts. This thesis illustrates the working mechanism of S-RuM technology first, and then introduces S-RuM passive electronic devices for radio frequency (RF) application. Current approaches to improve RF passive device performance are discussed. Designs of capacitors and filters based on S-RuM are demonstrated, followed by simulation and lab measurement results. Challenges associated with S-RuM passive electronics are addressed and solutions are proposed. Future work and potential wearable device applications are summarized.

Acknowledgments

To people close to me, for their continuous love and support.

Contents

1. Introduction

On-chip passive devices, including inductors, capacitors, filters, transformers, etc., are critical radio frequency integrated circuit (RFIC) components. Current on-chip lumped passive devices are designed based on a standard two-dimensional (2D) planar fabrication process, which limits their design in a 2D plane. This limitation inevitably gives the lumped passive devices huge footprints such that they occupy a significant portion of chip area. Furthermore, the large overlap with the substrate introduces serious substrate parasitic effects, which significantly increase energy loss and limit applicable maximum frequency [1]. Efforts have been made for a long time to shrink their size and improve performance. However, technologies like multiple layer 2D processing, 3D MEMS and chemical modification of substrates only address some aspects of the major issues with 2D device structures [2-5]. Recently, in our lab, we have demonstrated a novel on-chip design platform for lumped passive components based on self-rolled-up membrane (S-RuM) tubular structures [6, 7]. By applying the concept of processing in 2D and functioning in 3D via a deterministic self-assembly mechanism, this platform allows designers to bypass mechanical stability issues associated with traditional 3D structures, and changes fundamentally the tradeoff between device performance and on-chip footprint. Preliminary success has been obtained on designing and experimentally demonstrating some of the key passive RFIC components including inductors and transformers [8, 9]. For example, we have demonstrated rolled-up inductors with as much as 100x size reduction compared to their planar counterparts, while exceeding the operation frequency of the-state-of-the-art planar inductors. Moreover, the stable electromagnetic confinement and miniaturized footprint make these devices inherently compatible with flexible substrates and wearable technologies. Through structured transfer-printing or multi-level sacrificial layer releasing, high density integration of discrete rolled-up components can be achieved. This thesis focuses on S-RuM technology to realize two other essential RFIC passive devices: capacitors and filters. Together with S-RuM inductors

and transformers, it is clear that passive RFIC electronics can be realized on a 3D platform that is extremely area and weight efficient, high performance, and robust.

1.1 Self-rolled-up membrane (S-RuM) technology

S-RuM tubes are formed by releasing energy built up in strained planar membranes. This process was first discovered by Prinz *et al.* in 2000 [10]. As shown in Figure 1, the InAs layer is compressively strained when deposited on GaAs substrate pseudomorphically [11]. Upon release from the AlAs sacrificial layer, the InAs layer tends to expand, while the GaAs layer resists such expansion. The oppositely oriented forces of the bilayers generate a momentum that is perpendicular to the thin film plane, and drive the planar membrane to scroll up and continue to roll into a tubular spiral structure. The uniqueness of the tubular structure quickly drew the attention of researchers, and many studies on different strained thin film systems have been carried out. Rolled-up tubes formed by epitaxial single-crystal films, metal thin films, amorphous dielectric films, strained polymer bilayers, and hybrid material films have been demonstrated [12],[13],[14]. Among them, we found that dielectric film tubes show great potential for realizing novel RF passive devices for their electromagnetic properties. Inductors, transformers, capacitors, and filters based on S-RuM technology are realized in our lab.

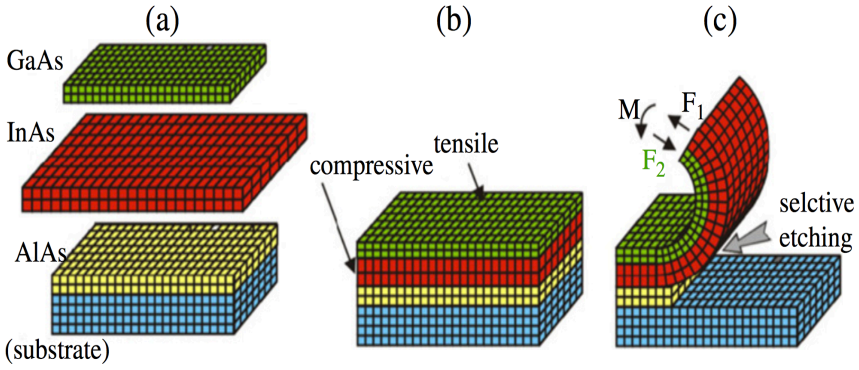

Figure 1 Schematic of deformation of strain-induced membranes. (a) Ga/As bilayer structure with AlAs as the sacrificial layer. (b) The bilayer is deposited pseudomorphically on the substrate. InAs experiences compressive strain and GaAs experiences tensile strain. (c) Selectively removing AlAs sacrificial layer releases the bilayer, and a net momentum from the opposite force from each of the bilayers drives the membrane to scroll up and roll into tubes.

S-RuM platform for RF passive electronics is based on a strained SiNx bilayer system and engineered conducting layer. SiNx film is CMOS processing technology compatible, and is often used as a gate dielectric material for transistors. The fabrication of SiNx thin films is completed by a dual-frequency plasma enhanced chemical vapor deposition (PECVD) system in an ammonia (NH_3)/silane (SiH_4)/nitrogen (N_2) environment. N-H, Si-H, and Si-N bonds coexist in the deposited SiNx thin film, and the content of bonded hydrogen (NHx and SiH) determines the residual stress of the thin film [15]. At high frequency (13.56 MHz), the content of bonded hydrogen is rich and thus the deposited thin film shows strong tensile stress. The tensile stress can be increased from 200 MPa to 400 MPa as the NH_3/SiH_4 ratio increases. Low frequency (380 kHz) causes the stress state change from tensile to compressive. The high-energy ion bombardment that occurs through the low frequency is responsible for the compressive stress of the deposited film [16]. The densification of the film caused by the ion bombardment causes the film to expand against its volume and hence results in a compressive stress. Low pressure enhances compressive stress by providing a longer mean-free-path for radicals in the plasma, allowing more to reach the surface, and thus creates a denser and more compressively strained film. For many RF passive electronics applications based on the S-RuM platform, it is desirable to achieve small tube inner diameter so the area miniaturization and EM coupling efficiency can be optimized. This requires that the stress in the thin films should be as large as possible. In practice, the thin film stress is tuned so that it is large but not too extreme to cause pinhole issue. The residual stresses are measured, using a FSM 500TC, to -1168 and 406.9 MPa for the LF and HF SiNx thin film, respectively.

RF passive devices can be realized when a predefined conducting pattern rolls up together with the strained dielectric SiNx bilayer. A wide range of conducting materials are compatible with S-RuM technology. Gold (Au) and copper (Cu) are two good candidates for their high conductivity and low Young's modulus. Low Young's modulus is ideal since it has an inverse proportional relation with the

rolled-up tube inner diameter. It should be noted that 2D materials, including graphene and MoS_2, are particularly suitable to act as the conducting layer in S-RuM devices. Their high conductivity and mono-atomic nature make the rolled-up tubular devices extremely compact and powerful.

1.2 S-RuM devices for radio frequency (RF) application

The S-RuM platform provides a universal solution to break the bottleneck of current RFIC passive electronics. It is a promising technology to meet the requirement for higher data rate, energy efficient, and portable communication. This section demonstrates S-RuM inductors and transformers that are already realized in our lab.

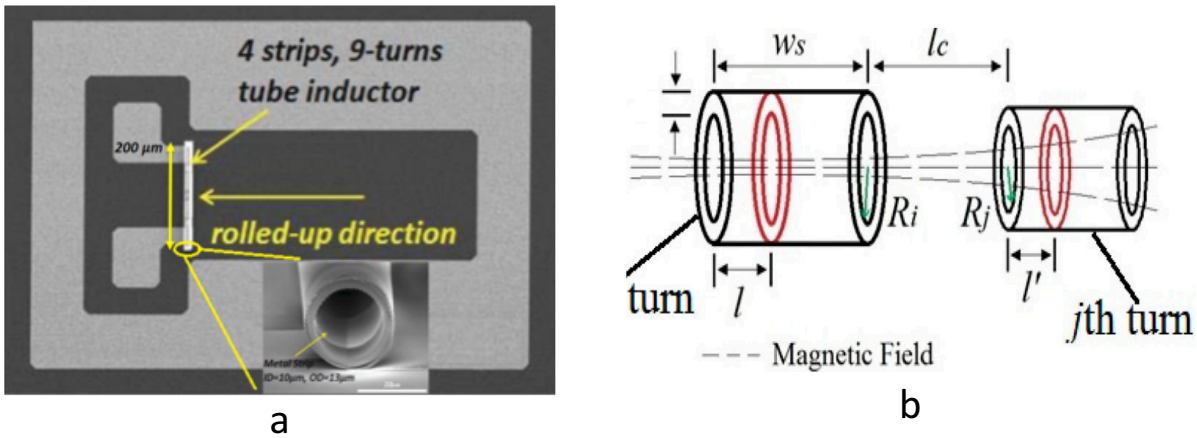

Figure 2 S-RuM inductors. (a) SEM picture of a 4-strips 9-turn tube. (b) Magnetic coupling in any adjacent cells.

1.2.1 S-RuM inductors

Inductors are widely used in RFIC as RF choke, matching element, and filtering element. We have used the self-rolled-up membrane platform to roll up the predefined square wave-like conductive layer into 3D multiple-turn spirals and build high-performance rolled-up inductors, as shown in Figure 2(a). When AC current flows in and out of the feed lines, a time-varying EM field is triggered. The spirals can be treated electrically as multilayer closed concentric cylinders as shown in Figure 2(b). This 3D structure has the ability to significantly better confine an electromagnetic (EM) field compared to conventional planar spiral on-chip inductors. Much enhanced mutual magnetic coupling between turns in spirals can be obtained. Rolled-up geometry also avoids a large portion of EM field being distributed in the

substrate and therefore dramatically reduces the substrate parasitic effects, making its electrical performance independent of substrate. In the simulation shown in Figure 3(a), with 100 nm thick, 30 nm wide Cu layer and 9 µm inner diameter, more than 100× reduction in footprint can be realized using this platform while achieving excellent electrical performance, including large inductance, high quality (Q) factor ~ 20 at 8 GHz, and high self-resonance frequency (f_0) into Ku band. With a four-layer graphene conductive layer, tube inductors can further reach Q factor as high as 27 at 18 GHz. Figure 3(b) shows the preliminary results and HFSS simulated performance, the two of which are consistent, of a set of fabricated tube inductors with 100 nm gold conductive layer.

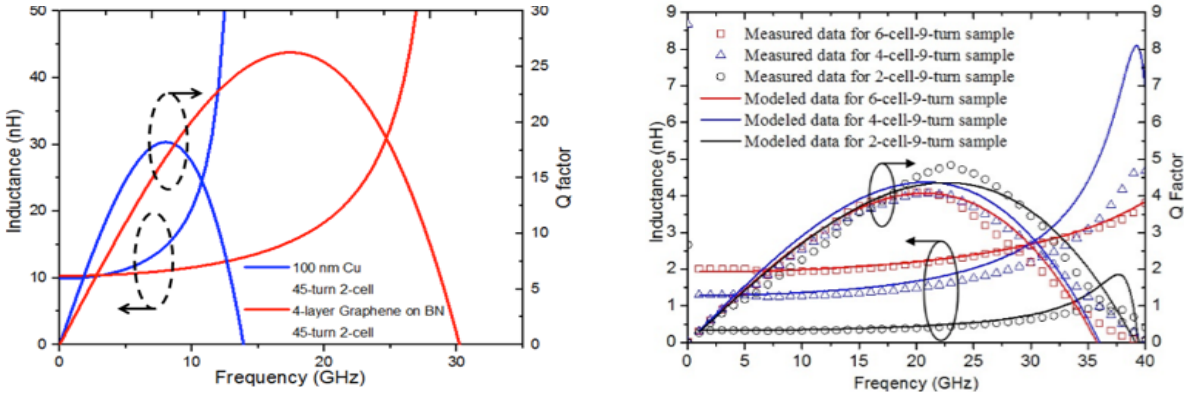

Figure 3 Tube inductor performances. (a) Measured inductance and Q factor of a four-cell tube inductor with different number of turns showing excellent performance up to millimeter wave range. (b) Comparison between the experimental and modeled data for various geometries.

1.2.2 S-RuM transformers

Transformers are essential in many RFIC systems. The functions include but are not limited to voltage transformation, DC-DC and AC-DC transform, and impedance matching. Like other S-RuM RF passive devices, S-RuM transformers utilize the concept of 'process in 2D and function in 3D'. The primary strips can be totally wrapped inside the secondary strips after the device rolled up. The voltage transform coefficient equals the turn ratio of primary and secondary strips. No matter what turn ratio is desired, the coupling coefficient k which is determined by the magnetic flux shared by the primary and

secondary windings in the center part can almost equal one. This is beyond the limit of 2D-structured transformers. Table 1 compares the performance of a tube transformer design to the best reported on-chip planar transformer with the same turn ratio n. The area density of the product of n and k of the tube transformer is more than 15x larger than that of the planar transformer with 12x smaller footprint.

Table 1 Comparison between sample and the best planar transformer

Device	Chip Area (μm^2)	Lp/Area (nH/mm^2)	Ls/Area (nH/mm^2)	k	n	nxk/Area ($1/mm^2$)
Sample A	805	627.3	40.6	0.89	5.5	6046
Planar	10000	1052	34	0.7	5.59	391

2. Literature Review

Researchers have been working for decades to improve the performance of RF on-chip passive devices, and much progress has been demonstrated. For RF on-chip capacitors, the major bottleneck is capacitance density. To improve capacitance density, decreasing dielectric layer thickness and using high-k material are commonly adopted. Both methods trade off overall leakage current, breakdown voltage, and voltage linearity. In this chapter, three approaches to improve capacitance density, with little compromise of other technical specs, are summarized.

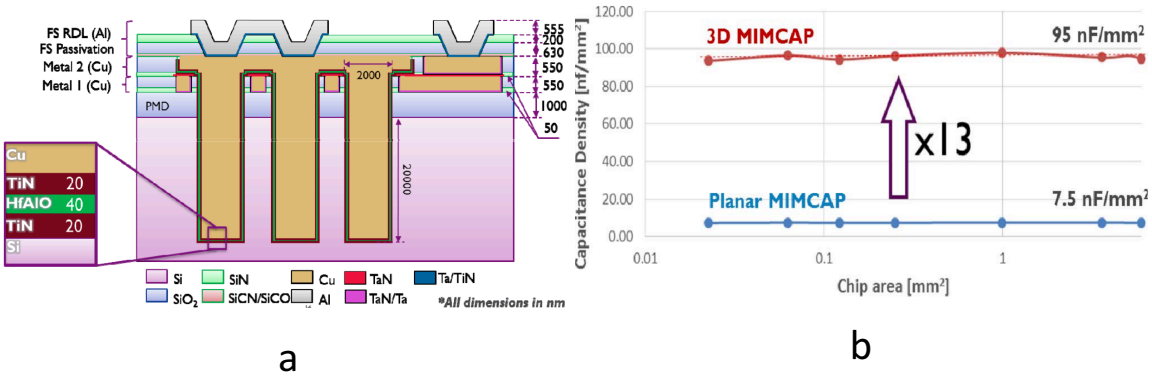

Figure 4 3D MIM capacitor. (a) Schematic cross-section of 3D MIM capacitor technology. (b) Capacitance density as a function of chip area for planar and embedded 3D MIM capacitors.

Neve et al. showed that by fabricating an embedded 3D MIM capacitor on a Si interposer, capacitance densities can reach as high as 96 nF/mm^2 [17]. The 3D capacitors are realized by etching 20 µm-depth TSV-like holes after Metal 1 Cu deposition. ALD deposition of a TiN/HfAlO/TiN (40/20/20 nm-thick) layer and Metal 2 Cu plating follow. This process is shown in Figure 4(a). The effective capacitance area is greatly increased from 7.5 to 96 nF/mm^2 as shown in Figure 4(b).

To improve capacitor performance, Bharti and Tiwari introduced the use of a dielectric stack consisting of three layers in which the middle layer is deposited at a higher temperature than the top and bottom layers [18]. The principle behind this approach is that higher dielectric roughness increases

the capacitance density. Roughness of the top and bottom interfaces of the dielectric layer increases the average electric field in the insulator film, and also increases the effective contact area.

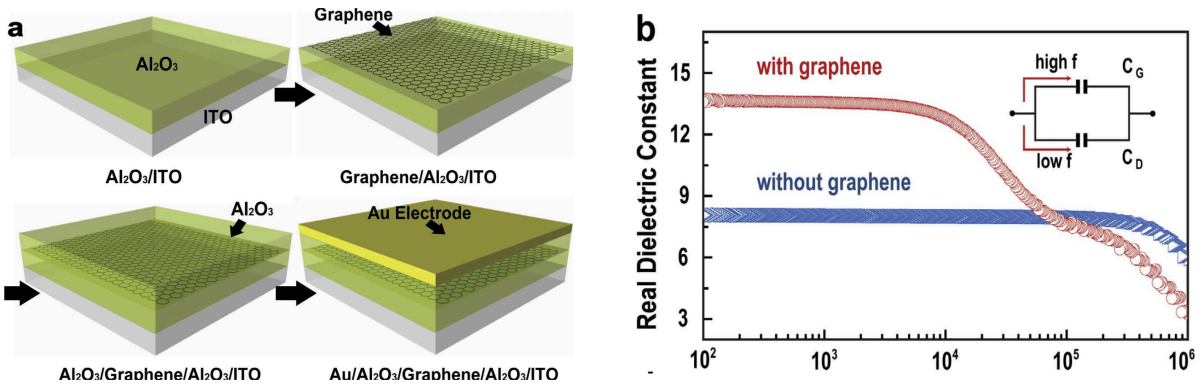

Figure 5 Graphene-embedded dielectric capacitors. (a) Schematic of the graphene-embedded Al2O3 capacitor fabrication process. (b) Real dielectric constant as a function of frequency. Inset is the equivalent circuit.

Min et al. demonstrated that by embedding graphene in Al_2O_3 dielectric, electrical double layer (EDL) capacitors can be formed, thus increasing the effective permittivity of the dielectric layer [19]. As shown in Figure 5, Al_2O_3 was deposited on an ITO plate. A CVD grown graphene layer was transferred on top of Al_2O_3 through PMMA. Au was deposited on the top to function as the capacitor top plate. The authors claim that the local internal fields are enhanced by space charge polarization, so a set of EDLs is created at the graphene-Al_2O_3 interface. The total capacitance is thus governed by the EDLs at lower frequency, and is the main factor for the increased effective dielectric constant. The authors also tried to increase the number of graphene layers and found that three graphene inter-layers are the optimal structure. This is because hole concentration with three graphene layers is at a maximum. More layers do not provide more holes due to saturation and may affect dielectric layer quality.

3. Description of Research Results

3.1 S-RuM capacitors

Capacitors in RFIC play multiple roles including but not limited to impedance matching, voltage and current transforming, phase shifting, direct current (DC) blocking, and energy storage. Many of these functions require large capacitance value, inevitably making the capacitors utilizing traditional two-dimensional (2D) metal-insulator-metal (MIM) structure very large. The large on-wafer foot-print also introduces parasitics which can cause performance drift and degradation. A tremendous amount of work has been done to shrink the size of capacitors, including decreasing dielectric layer thickness and using high-k dielectric material [20],[21]. However, these efforts trade off other figures of merit including leakage current, breakdown voltage, and cost. We developed a technology of rolled-up 3D ultra-compact capacitor which fundamentally breaks the capacitance density limit of planar devices and is compatible with wearable electronics. By releasing the strain built up in a SiNx bilayer though etching away the sacrificial layer beneath it, metal plates start to scroll up together with the high-k dielectric layer in between. The thin films continue to roll as the removal of the sacrificial layer takes place forming a multiple-turn structure. The entire device only has a footprint equal to the projection area of the tubular structure. This footprint barely increases as the number of turns keeps growing. Ultra-high capacitance density can thus be achieved.

3.1.1 Design of S-RuM capacitors and fabrication process

The approach we used to achieve a rolled-up multi-spiral tubular structure relied on strain releasing. Twenty nm low frequency (360 kHz) PECVD deposited SiNx and 20 nm high frequency (13.56 MHz) PECVD deposited SiNx form the strained bilayer thin film on top of a germanium sacrificial layer. The sacrificial layer can be deposited on any rigid or flexible substrate. By releasing the sacrificial layer through XF_2 dry etch or H_2O_2 wet etch, the opposite strain built up in the bilayer releases and generates a momentum perpendicular to the thin film plane. This momentum drives the bilayer, together with the

MIM part thin film on the top, to roll into a multi-spiral structure. The MIM layer consists of high-k dielectric such as SiNx, and is sandwiched by thermal evaporated gold conducting plates. The thickness of the SiNx dielectric layer is set to be 20 nm to withstand high breakdown voltage, while increasing capacitance density. The thickness of the metal plates is set to 60 nm each for the consideration of small rolled-up inner diameter.

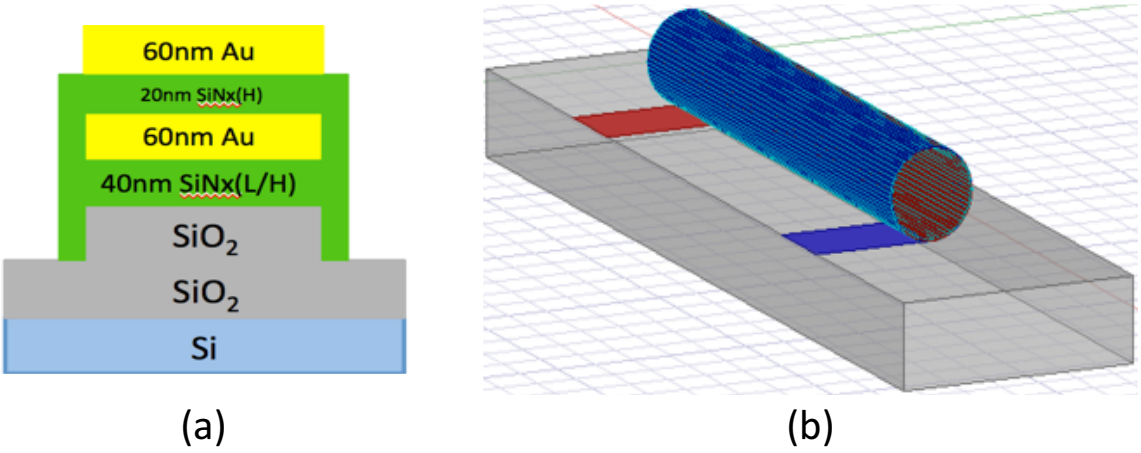

Figure 6 Structure of SiNx based rolled-up capacitors. (a) Layer construction diagram of the capacitor. (b) Rolled-up capacitor model in electromagnetic simulator HFSS.

3.1.2 S-RuM capacitors simulation results

The structure of the device is shown in Figure 6(a), and the model for the device in the electromagnetic (EM) simulator is shown in Figure 6(b). We can observe from Figure 7 that the capacitance increases fast from one turn (Figure 7(a)) to three turns (Figure 7(b)), and three turns provide 168.8 pF at 1 GHz, satisfying the design goal. We can also observe that the inductance associated with the tubular capacitor is significant due to the strong magnetic field along the axial, generated by the concentric metal cylinders. The capacitance of the three-turn device starts to take off at 1.4 GHz, and the device is resonant at 1.6 GHz. This should be taken into consideration in circuit design.

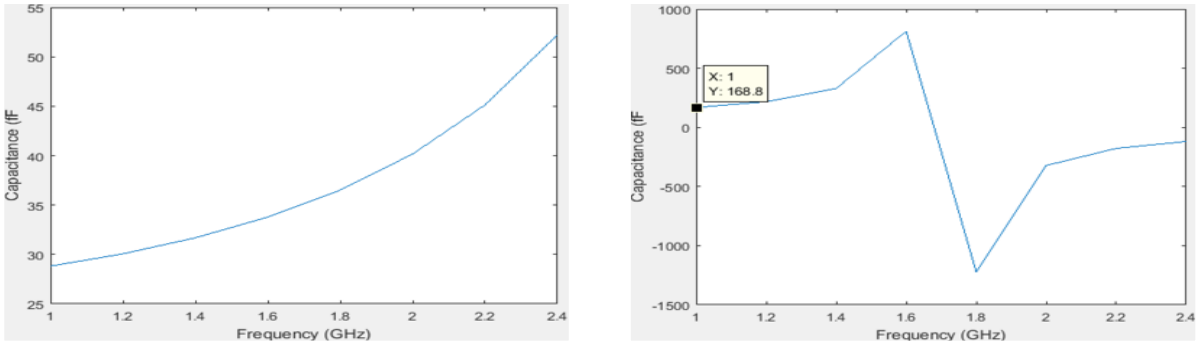

Figure 7 Simulation results of rolled-up capacitors. (a) Capacitance versus frequency for one-turn capacitor. (b) Capacitance versus frequency for three-turn capacitors. Both devices have axial plate dimension of 140 µm.

3.2 S-RuM filters

Filters are essential RF components in heterodyne transceivers to select target frequency spectrum and suppress spectral components at image frequencies. Although being researched for decades, the state-of-the-art technologies have serious bottlenecks that are difficult to circumvent. First, lumped element filters cannot be used at frequencies above X band (~ 7.0 to 11.2 GHz), and distributed filters suffer from large footprint and are therefore hard to integrate on-chip monolithically [22]. In addition, their performance is severely affected by substrate loss caused by electric and magnetic coupling between the resonator and the lossy substrate.

Filters based on SiNx self-rolled-up nanomembrane technology combine the advantages of lumped element filters and distributed filters, and have strong immunity to substrate effects due to the extremely small footprint and minimized parasitic coupling. As we will show in the following, the rolled-up filters can realize all-frequency-band design on any substrates up to 80 GHz. The excellent properties of tube filters come from the concept of 'processing in 2D and function like 3D' enabled by strain engineering. By designing the pattern layout of the conductive layer on top of the strained SiNx bilayer in a 2-D plane, inductors and capacitors with different terminations can be integrated monolithically in one compact 3-D tube structure after rolling up. Low pass, high pass, and band pass filters with high

electrical performance can thus be designed using the tubular lumped structure resonators realized by this S-RUM technology.

3.2.1 Design of S-RuM filters and fabrication process

SiNx self-rolled-up membrane tubular filters form spontaneously when strained planar membranes deform as a result of energy relaxation. The strained membrane includes a patterned conductive layer on an oppositely strained SiNx bilayer, which is in contact with a germanium sacrificial interlayer on a substrate. The deposition method and properties of the SiNx bilayer are discussed in Chapter 1.

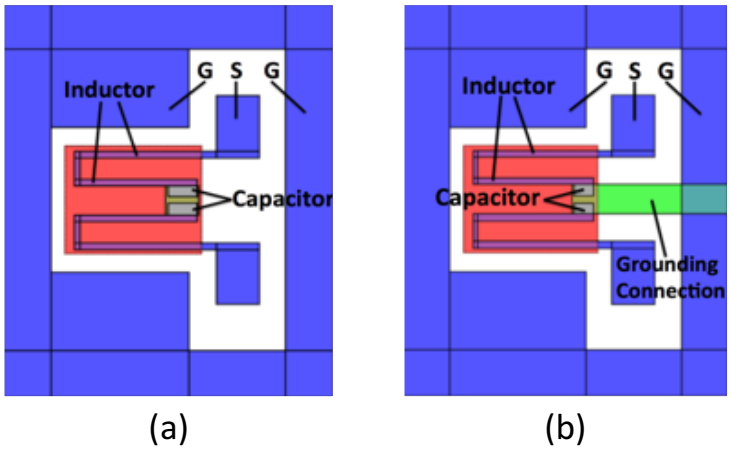

Figure 8 Layout of tubular resonators before roll-up. (a) Series LC resonator. (b) Parallel LC resonator.

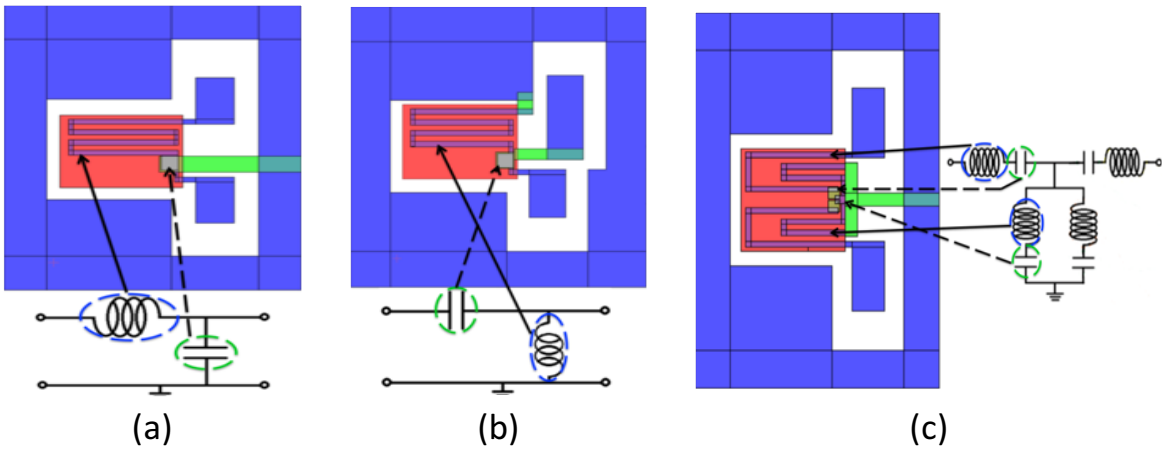

Figure 9 Layout of different types of tubular filters. (a) Low pass filter. (b) High pass filter. (c) Band pass filter.

The conductive pattern layer, with a thickness ranging from tens to a few hundreds of nanometer, on the strained SiNx layer is the active part providing the filtering function upon roll-up. Materials that can be selectively etched from SiNx and have high conductivity can be used for this layer, and include but are not limited to gold, copper, silver, and graphene. The design of the conductive layer pattern follows the design principles of the lumped structure filter. The order number of the filter determines the number of LC resonators in the filter structure. The increased order number improves the stop band attenuation rate at the expense of greater insertion loss. This loss is more pronounced in S-RuM filters due to higher resistivity of thin film compared to bulk material. As shown in Figure 8, a rolled-up tubular resonator is formed by combination of inductor and capacitor in series or shunt connection. The serpentine conducting strips form tightly coupled co-axial multi-layer spirals after being rolled up and function as a rolled-up tubular inductor as AC signal flows through. The conducting plates, together with the dielectric material in between, form a rolled-up tubular capacitor. By varying the length and width of the serpentine strips and dimension of conducting plates, different values of inductance and capacitance can be achieved, determining the resonator's resonant frequency (f0) and thus the pass band frequency of the band pass filter, and cut-off frequency of low pass and high pass filter. As shown in Figure 9, the layout of the resonators determines the type of the filter. Figure 9(a) shows the design of a low pass filter with cutoff frequency at 3 GHz. The length of the serpentine strip is 270 μm and width is 15 μm. With an inner diameter of 9 μm upon roll-up, the serpentine line forms a 9-turn spiral inductor with inductance of 0.8 nH. The 20 μm x 20 μm dimension plates provide conductance of 132 fF at 5 GHz. Figure 9(b) shows the design of a high pass filter with cutoff frequency at 6 GHz. Figure 9(c) shows a band pass filter with 8-turn inductor in the series branch and 3-turn inductor in the shunt branch. A common ground is created to realize shunt connection of the rolled-up inductor and capacitor. The footprint of this tubular structure is only 10 μm x 210 μm, less than one hundredth the size of the best reported result [23]. Figure 10 shows the SEM pictures of tubular filters before being rolled up.

Benefiting from the 'process in 2D and function in 3D concept', the tubular filter saves a tremendous amount of precious wafer area and minimizes the parasitic coupling introduced by the lossy substrate.

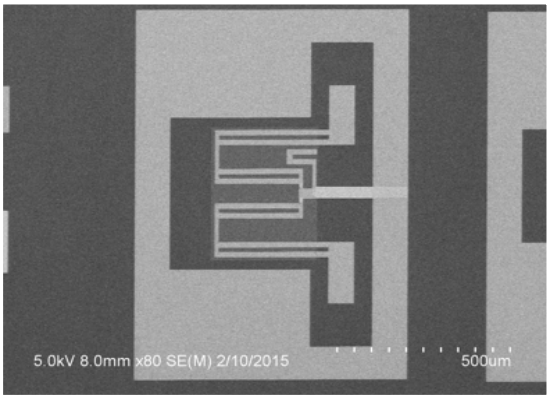

Figure 10 SEM of tubular band pass filter before roll-up.

3.2.2 S-RuM filters simulation results

In order to precisely predict the performance of rolled-up filters, physical model and equivalent circuit model are both used to perform the structure design. Physical model is built based on the low-pass filter prototype model, and the values of the rolled-up inductor and capacitor elements are calculated by analytical methods. For the rolled-up inductor, inductance $L_{resonator}$ is governed by:

$$L_{resonator} = \frac{N[R^2 + \omega^2(L')^2]\{L' - C[R^2 + \omega^2(L')^2]\}}{R^2 + \omega^2\{L' - C[R^2 + \omega^2(L')^2]\}^2}$$

where N is the number of spiral turns, C is the parasitic capacitance value of the spiral inductor, $L' = L - 2(1 - N^{-1})M$, with M being the mutual inductance between adjacent spirals and L being the self-inductance of one spiral turn [9]. For the rolled-up capacitor, capacitance $C_{resonator}$ is governed by:

$$C_{resonator} = \frac{C_0}{1 - \omega^2 L_{resonator\_1turn} C_0}$$

where $C_0 = \mu_r \mu_0 A t_{dielectric}^{-1}$ is the capacitor's value of MIM planar capacitor with the same plate dimension. Unwanted crosstalk capacitances are taken into account in the design by building up the

lumped circuit model in commercial software ADS. Figure 11(a) indicates such an example of a tubular band pass filter design. An optimization method can then be used to find the best value of all parameters to finalize the structure design. Accuracy of the roll-up control is governed by FEM modeling.

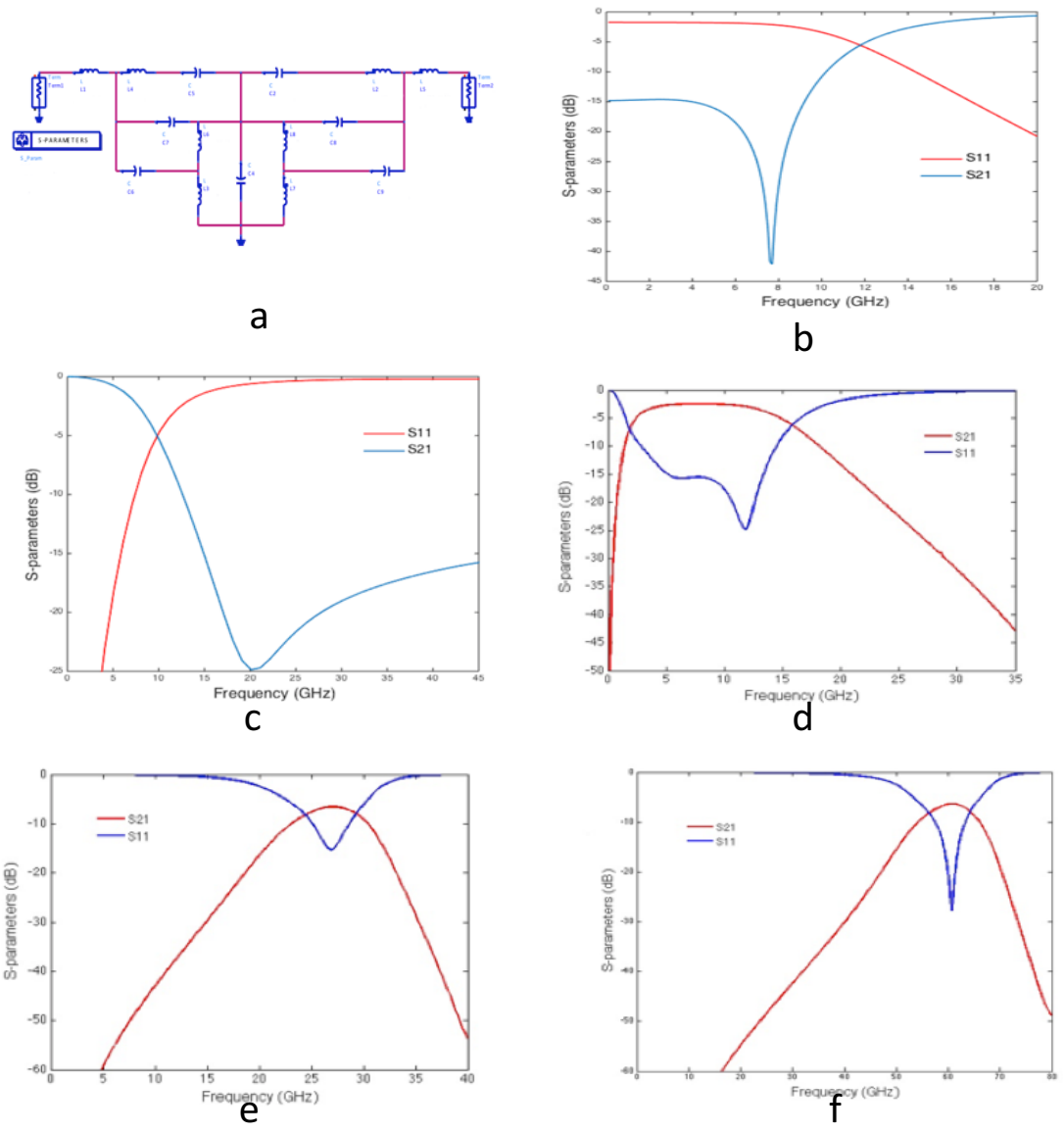

Figure 11 Tubular filter simulations. (a) Model schematic of optimizing tubular band pass filter. (b) Low pass filter with cut-off frequency at 8 GHz. (c) High pass filter with cut-off frequency at 15 GHz. (d) Band pass filter with center frequency at 8.5 GHz. (e) Band pass filter with center frequency at 26 GHz. (f) Band pass filter with center frequency at 60 GHz.

Figure 11 shows the simulation results of several tube filters designed for different application scenarios in important frequency bands. Figure 11(b) shows a low pass tube filter working up to 8 GHz with return loss -18 dB and insertion loss -2 dB. Figure 11(c) shows a high pass tube filter working up to 15 GHz with return loss -17 dB and insertion loss -1.5 dB. Figure 11(d) shows a wide band pass tube filter working in X band from 5 GHz to 12 GHz with return loss -15 dB and insertion loss -2.5 dB. Figure 11(e) shows a band pass tube filter working in K band from 25 GHz to 27 GHz with return loss -18 dB and insertion loss -8 dB. Figure 11(f) shows a band pass tube filter working in U/E band from 59 GHz to 61 GHz with return loss -18 dB and insertion loss -7 dB. All the filters are made by 100 nm Au metal strips. Compared to the smallest lumped on-chip filters so far, the tube filters have footprint in the range of 10 x 200 μm^2, which is more than 70 times smaller than that of their counterparts.

3.2.3 S-RuM filters applications

With its extremely compact size, high frequency and ultra-wide-band operation capability, this novel filter platform has many promising applications. One potential market is in high data rate communication portable devices. When working in unlicensed spectrum around 10 GHz or 60 GHz, the ultra-compact tube based filters can be designed with bandwidth more than 5 GHz, making the data transmission speed as high as several gigabytes per second. Popular next-generation high speed technologies like portable wireless high definition (WirelessHD) display, high speed wireless big data synchronization, download, and storage on portable devices can definitely benefit from the excellent properties of tube-based filters. The compact size of the tube filters also makes them good candidates for home automation. Small appliances like LED bulbs can be connected to wireless local area networks (WLANs) using WiFi chips with S-RUM filters. What is more promising is that the tube filters are perfectly compatible with wearable electronics technology. Unlike the filters based on 2D processing, the electromagnetic field confined inside the tubular structure does not change with the deformation of the substrate. This uniqueness together with the extremely small footprint enable the tube filters to be

used on flexible substrates or rigid substrates with huge strain and large curvature. Potential applications can be found in wearable computing electronics like smart glasses and wristwatches, body-centric communication systems, wireless sensors for medical imaging and positioning, and wireless body area networks (WBANs).

4. Challenges and Strategies

The SiNx pinhole issue is the root cause of many of the device malfunction issues. The pinhole comes from the large stress built up in the SiNx bilayer [24]. The thin film is not robust enough to withhold the large stress. Since the pinholes are at the bottom layer, every layer deposited on top of SiNx is affected, and the discontinuity transfers to the very top layer if the MIM sandwich is not thicker than the SiNx layer. In the case where the metal layers are thick, the pinhole is filled by metal and forms a metal bump. The distance between the tip of the bump and the top plate is much smaller than the dielectric layer thickness, leading to a larger capacitance value. In the case where the metal layer is thin, the pinhole penetrates through the conducting plate and the device is thus open-circuited. To reduce the pinhole effect, one may adjust the NH_3/SiH_4 ratio to reduce the stress in the SiNx bilayer. The metal pattern on top of the SiNx can also be engineered to help distribute the stress and direct the pinhole to locations that are not sensitive to device performance.

Temperature stability is another major concern of S-RuM devices. Unlike devices with planar technology whose heat can be dissipated through the substrate, 3D tubular devices have the heat mostly confined in the structure. The reason is that the contacting area, or footprint, of the tubular capacitor is only the projection of the cavity. Since the deposition temperature for the SiNx strained layer is 300 ^{o}C, it is a rule of thumb that users keep the operational temperature below this point. Operational temperature higher than 300 ^{o}C may cause deformation of the SiNx layer and thus cause capacitance drift [25]. During the test we found that the SiNx started to expand at 350 ^{o}C. Since the inner layer has higher temperature than the outer layer, the deformation caused the metal plates to clap and caused short circuit. A strategy to avoid heat accumulation is to fill the tubular cavity with thermal conductive material like nickel powder paste. Metal powder has much better heat conductivity than vacuum and air, and can boost permeability of the core area and thus increase device Q factor.

The Q factor of the tubular capacitor depends heavily on the resistivity of the metal plate. The

resistivity of thin film is higher than that of the bulk material due to increased surface interactions as well as absorption of conduction electron and scattering effects [26]. These effects are more pronounced when the operation frequency is high. To minimize thin film resistivity, one approach is to improve thin film quality. By slowing the metal deposition speed, the metal thin film is smoother. Scattering effect can thus be reduced.

Cu is an ideal choice for the metal plate. The low Young's modulus gives tube devices with Cu small inner diameter, which is key to improving capacitance density. Cu also has low resistivity, and is fully compatible with CMOS technology. The drawback of Cu is that it is easily oxidized at high temperature when the environment is not moisture free. Unfortunately, the method to etch away the sacrificial layer always requires oxidizer and is usually solution based (like hydrogen peroxide). An approach to protect Cu from oxidization is to use a protection layer such as aluminum oxide. The solution based oxidizer thus will interact with the sacrificial layer only. It is worth noting that contacts are still required in order to feed AC signal into the device and get output. So an additional lithography processing step is needed to define the window for production layer exposure. An oxidization resilient metal like nickel can be used to cover the copper layer underneath.

5. Future Work and Conclusion

Rolled-up capacitors with ultra-high capacitance density and rolled-up filters based on strain induced bilayer releasing are achieved. Simulation results show promising device performance and provide insight into device structure design. This technology shows great potential to be utilized in commercial portable electronics, as well as in wearable electronics. Several challenges and the way to improve device performance are discussed in this study.

References

[1] C. P. Yue and S. S. Wong, "Physical modeling of spiral inductors on silicon," *IEEE Transactions on Electron Devices,* vol. 47, pp. 560-568, 2000.

[2] C.-C. Tang, C.-H. Wu, and S.-I. Liu, "Miniature 3-D inductors in standard CMOS process," *IEEE Journal of Solid-State Circuits,* vol. 37, pp. 471-480, 2002.

[3] M. M. Ali, B. Bycraft, C. Schlosser, B. Assadsangabi, and K. Takahata, "Out-of-plane spiral-coil inductor self-assembled by locally controlled bimorph actuation," *Micro & Nano Letters,* vol. 6, pp. 1016-1018, 2011.

[4] C.-H. Jan, M. Agostinelli, M. Buehler, Z.-P. Chen, S.-J. Choi, G. Curello*, et al.*, "A 32nm SoC platform technology with 2nd generation high-k/metal gate transistors optimized for ultra low power, high performance, and high density product applications," *IEEE International Electron Devices Meeting (IEDM),* pp. 1-4, 2009.

[5] C.-M. Nam and Y.-S. Kwon, "High-performance planar inductor on thick oxidized porous silicon (OPS) substrate," *Microwave and Guided Wave Letters,* vol. 7, pp. 236-238, 1997.

[6] X. Li, "Strain induced semiconductor nanotubes: from formation process to device applications," *Journal of Physics D: Applied Physics,* vol. 41, p. 193001, 2008.

[7] X. Li, "Self-rolled-up microtube ring resonators: a review of geometrical and resonant properties," *Advances in Optics and Photonics,* vol. 3, pp. 366-387, 2011.

[8] W. Huang, X. Yu, P. Froeter, R. Xu, P. Ferreira, and X. Li, "On-chip inductors with self-rolled-up SiNx nanomembrane tubes: A novel design platform for extreme miniaturization," *Nano letters,* vol. 12, pp. 6283-6288, 2012.

[9] W. Huang, M. Li, S. Gong, and X. Li, "Self-rolled-up tube transformers: Extreme miniaturization and performance enhancement," *Device Research Conference*, pp. 223-224, 2015.

[10] V. Y. Prinz, V. A. Seleznev, A. K. Gutakovsky, V. V. preobrazhenskii, and T. A. Gavrilova, "Free-standing and overgrown InGaAs/GaAs nanotubes, nanohelics and their aarrays," *Physics E*, vol. 6, pp. 828-831, 2000.

[11] X. Li, "Self-rolled-up microtube ring resonators: a review of geometrical and resonant properties," *Advances in Optics and Photonics*, vol. 3, pp. 366-387.

[12] Y. Mei *et al.*, "Versatile approach for integrative and functionalized tubes by strain engineering of nanomembrane on polymers," *Advanced Materials*, vol. 20, no. 21, pp. 4085-4090, 2008.

[13] W. J. Arora, A. J. Nichol, H. I. Smith, and G. Barbastathis, "Membrane folding to achieve three-dimentional nanostructures: nanopatterned silicon nitride folded with stressed chromium hinges," *Applied Physics Letters*, vol. 88, no. 5, p. 053108, 2006.

[14] A. Rottler et al., "Rolled-up nanotechnology for the fabrication of three-dimentional fisgnet-type GaAs-metal metamaterials with negative refractive index at near-infrad frequencies," *Applied Physics Letters*, vol. 100, no. 15, p. 151104, 2012.

[15] O. Semenova, A. Kozelskaya, L. Z. Yong, and Y. Y. De, "Mechanical strains in PECVD SiNx:H films for nanophotonic applications," *Chinese Physics B*, vol. 24, no. 10, 2015.

[16] P. Proeter *et al.*, "3D hierarchical architectures based on self-rolled-up sillicon nitride membranes," *Nanotechnology*, vol. 24, p. 475301, 2013.

[17] C. Roda Neve et al., "High-density and low-leakage novel embedded 3D MIM capacitor on Si interposer," *IEEE International 3D System Integration Conference*, 2016

[18] D. Bharti and S. P. Tiwari, "Improved properties of MIM capacitors using ALD Al_2O_3 by multi-temperature technique," *IEEE International Conference on Nanotechnology*, pp. 1015-1018, 2015.

[19] B. K. Min et al., "Capacitance in a graphene-embedded Al_2O_3 gate dielectric," *Scientific Reports*, vol. 5, p. 16001, 2015.

[20] Y. Apki, and T. Kunitake, “Solution-based fabrication of high-k gate dielectric for next-generation metal-oxide semiconductor transistors,” *Adv. Mater*., vol. 16, no 16, pp. 1867-1904, 2001.
[21] G. D. Wilk, R. M. Wallace, and J. M. Anthony, “High-k gate dielectric: current status and materials properties,” *Applied Physics*, vol. 89, pp. 5243-5275, 2001.
[22] Z. Zhang, and X. Liao, “Micromachined passive bandpass filters based on GaAs monolithic microwave-integrated-circuit technology,” *IEEE Transaction on Electron Devices*, vol. 60, no. 1, pp. 221-228, 2013.
[23] Y. Chen and S. Chang, “A ultra-compact 77 GHz CMOS bandpass filter using grounded pedestal stepped-impedance stubs,” *Microwave Conference*, pp. 194-197, 2011.
[24] A. Ghadiri and K. Moez, “High-quality-factor active capacitors for millimeter-wave applications,” *IEEE Trans on Microwave Theory and Techs*, vol. 60, pp. 3710-3718, 2012.
[25] P. Froeter, Y. Huang, O. V. Cangellaris, and X. Li, “Toward intelligent synthetic neural circuit: Directing and accelerating neuron cell growth by self-rolled-up silicon nitride microtube array,” *ACS Nano*, vol. 8, p. 11108, 2014.
[26] M. Hsieh, D. Jair, and C. Lin, “Design and fabrication of the suspended high-Q spiral inductors with X-beams,” *Microsystem Technologies*, vol. 14, no. 7, pp. 903-907, 2008.